

# Stretching of Pet Films under Constant Load.

## II. Structural Analysis

G. LE BOURVELLEC and J. BEAUTEMPS, *Rhône-Poulenc  
Recherches-CRC, 85, Av. des Frères Perret, 69190 St Fons, France*

### Synopsis

The structure development of a PET film is studied during drawings under constant load. The evolution of crystallinity, amorphous orientation, and axial and planar birefringences is described along a deformation path. The influence of the stretching force and stretching temperature is also analysed.

### INTRODUCTION

In the flat film process, one of the steps is a drawing between rolls and it is usually followed by a transversal stretching in an oven.<sup>1</sup> Therefore, the knowledge of the structure of the film stretched between rolls is important because the stretchability in the transverse direction depends on the structure developed during the first drawing.

The structure of a PET film generated by a stretching between two rolls has been described in the past by various techniques like polarized fluorescence, birefringence, X-ray diffraction, infrared dichroism, and Raman scattering.<sup>2-7</sup> As this kind of stretching can be represented by a drawing under constant load,<sup>8</sup> one of the main parameters which controls the structure is the stretching force, but its influence has not been described.

In a previous paper,<sup>9</sup> the kinetics of deformation involved in stretchings under constant load have been defined and typical cases of drawing between rolls have been enhanced: quenching, short plateau, and long plateau. In this investigation, a structural analysis is performed for these three kinds of stretching simulated by drawings under a constant load. The structure of PET films is described along a deformation path. The influence of the stretching force and the temperature effects are also specified.

### EXPERIMENTAL

#### Samples Preparation

Amorphous isotropic PET films (thickness 150  $\mu\text{m}$ ), supplied by Rhône-Poulenc Films, were oriented on an apparatus developed in our laboratory,<sup>9</sup> i.e., a stretching machine operating at constant load. Two temperatures (80 and 97°C) have been investigated. Some samples were annealed under constant load. After stretching or annealing, each sample was air-quenched to avoid any further isothermal crystallization.

### Measurement of Orientations

By using an Abbe refractometer, in polarized light, it is possible to measure the refractive indices in the three principal directions:  $n_1$  in the stretching direction,  $n_2$  in the transverse direction, and  $n_3$  in the direction perpendicular to the plane of the film.

As explained in the previous paper,<sup>9</sup> because of the geometry of the stretching (at constant width), the symmetry of the samples is uniaxial planar. This means that the directions 2 and 3 are not equivalent:  $n_2 \neq n_3$ .

Therefore, the planar orientation of the chains can be described by the birefringence  $\Delta N_{23} = n_2 - n_3$ . The axial orientation is expressed by the usual birefringence  $\Delta N_{12} = n_1 - n_2$ . From this axial birefringence, the amorphous orientation  $F_a$  has been calculated by combining the two-phase model of Samuels<sup>10</sup> and the Gaylord model for crystalline orientation,  $F_c$ .<sup>11</sup> The Gaylord model is in good agreement with experimental data on PET<sup>12-17</sup>:

$$\Delta N_{12} = X\Delta c^0 F_c + (1 - X)\Delta a^0 F_a$$

with  $X$  = degree of crystallinity,  $\Delta c^0 = 0.22$ ,<sup>14,18</sup>  $\Delta a^0 = 0.22$ ,<sup>19</sup> and  $F_c = (\text{DR}^3 - 1)/(\text{DR}^3 + 2)$ , where DR = draw ratio.

### Density

The densities of the samples were estimated with the average refractive index obtained by refractometry. Moreover, for PET, De Vries and co-workers<sup>18</sup> found a linear relation between the density  $d$  and the average index  $\tilde{n}$ .

$$d = 4.047(\tilde{n}^2 - 1)/(\tilde{n}^2 + 2)$$

with  $d$  expressed in g/cm<sup>3</sup>. This relation is independent of the degree of crystallinity,  $X$ , and the level of orientation.

### Degree of Crystallinity

The degree of crystallinity,  $X$ , was determined by the relation

$$X = \frac{d - d_a}{d_c - d_a}$$

with  $d_c = 1.457$  g/cm<sup>3</sup> and  $d_a = 1.336$  g/cm<sup>3</sup>.<sup>20</sup>

It is well known<sup>21</sup> that crystallinity can be overestimated when it is calculated with values of density measured on oriented samples, because of the increase in density of the amorphous phase with the orientation of the chains. However, Nobbs et al.<sup>5</sup> showed that, up to a level of amorphous orientation equal to 0.4, the density of the amorphous phase of PET does not exceed 1.342, i.e., a variation less than 0.5%, which is negligible for the determination of crystallinity.

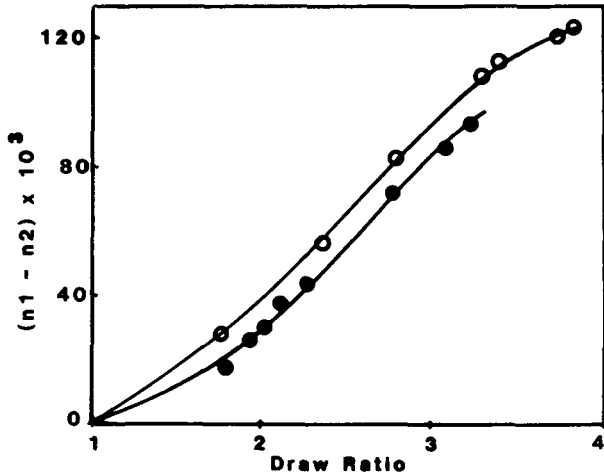


Fig. 1. Evolution of the axial birefringence during drawings at 80°C under various loads expressed in kg/mm<sup>2</sup>: (●) 0.50; (○) 0.75.

## RESULTS AND DISCUSSION

### Evolution of the Structure along a Deformation Path

Figure 1 shows the evolution of the axial birefringence with the draw ratio:  $n_1 - n_2$  gradually increases with the draw ratio and slightly increases with the stretching force. In Figure 2 are reported the variations of the planar birefringence  $n_2 - n_3$  with the draw ratio. The evolution is similar to this of the axial birefringence.

Figure 3 enhances the evolution of the degree of crystallinity with the draw ratio. Up to a critical draw ratio  $DR_c$ , no crystallinity is developed. For higher draw ratios than  $DR_c$ , the crystallinity increases with DR and is independent of the applied load.

However, as shown in Table I, the critical draw ratio depends on the load and decreases when the force increases. On the other hand, the birefringence

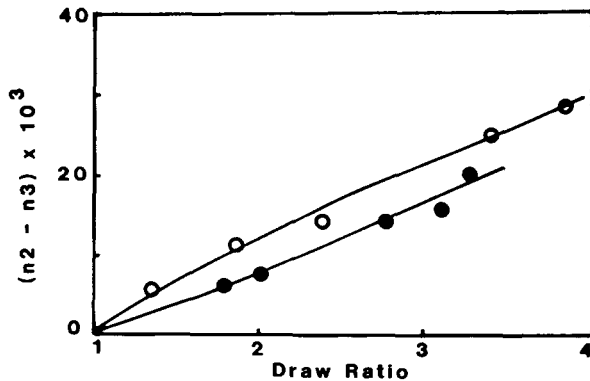


Fig. 2. Evolution of the planar birefringence during drawings at 80°C under various loads expressed in kg/mm<sup>2</sup>: (●) 0.50; (○) 0.75.

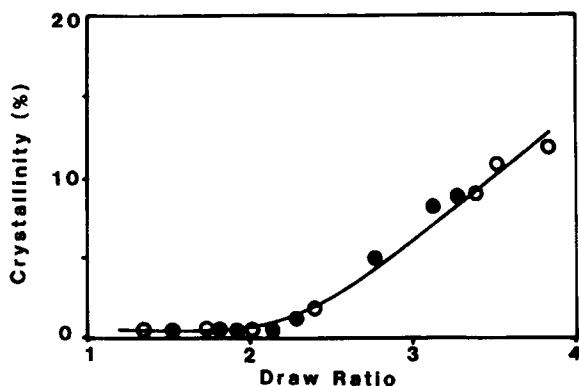


Fig. 3. Evolution of the crystallinity during drawings at 80°C under various loads expressed in kg/mm<sup>2</sup>: (●) 0.50; (○) 0.75.

associated with these critical draw ratios remains constant. Therefore, with this birefringence, it is possible to define a critical orientation for the induced crystallization, independently of the applied load, i.e., the strain rates spectrum (Table I). This result has already been observed in other experiments.<sup>22</sup> At a given temperature of stretching, the start-up of induced crystallization depends on a critical orientation which is independent on the strain rates spectrum which characterizes a path of deformation.

On each path of deformation, there is a draw ratio for which the strain rate takes a maximum value (Fig. 4). This draw ratio and the associated crystallinity have been reported in Table II for different stretchings at 80°C. This table shows that the point where the strain rate is maximum is located just after the beginning of induced crystallization. This observation can explain the fact that the kinetics of deformation slows down from this point. The small crystallites which appear act as tie points in the material, increasing its modulus. The deformation will stop at the plateau when an equilibrium is reached between stress, strain, and modulus.

### Influence of the Length of the Plateau

In a previous paper, short and long plateau stretchings have been enhanced for drawings between rolls.<sup>9</sup> In order to describe the effect of the length of the plateau, a few samples have been quenched at the beginning of the plateau and, others after a plateau of 30 s for stretchings at 97°C. During the plateau,

TABLE I  
Values of Critical Draw Ratio and Associated Axial Birefringence at the Startup of Induced Crystallization for Various Drawing Forces at 80°C

Stretching force (kg/mm <sup>2</sup> )	Critical draw ratio	Critical axial birefringence
0.50	2.15	0.037
0.63	2.10	0.035
0.75	2.00	0.036

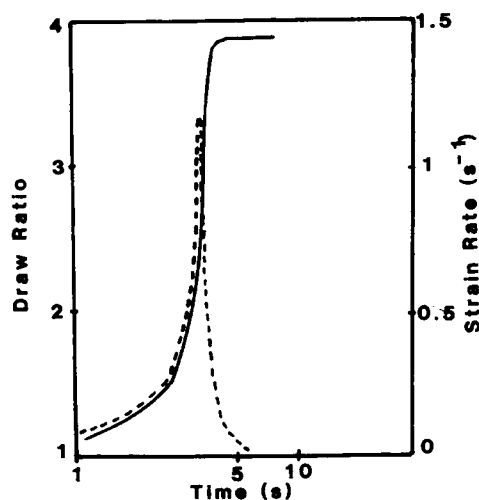


Fig. 4. Evolution of the draw ratio (solid line) and the strain rate (dashed curve) during a drawing at 80°C under 0.88 kg/mm<sup>2</sup>.

TABLE II  
Values of Draw Ratio and Associated Crystallinity at the Point of the  
Maximum Strain Rate for Various Drawing Forces at 80°C

Stretching force (kg/mm <sup>2</sup> )	Draw ratio at $\dot{\epsilon}$ maximum	Crystallinity (%)
0.50	2.4	2
0.63	2.2	1
0.75	2.4	2

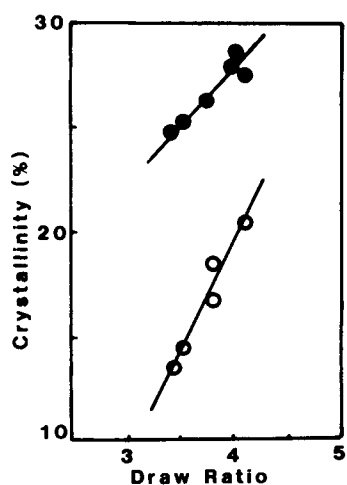


Fig. 5. Variation of the crystallinity with the plateau draw ratio at 97°C at the beginning of the plateau (O) and after a plateau of 30 s (●).

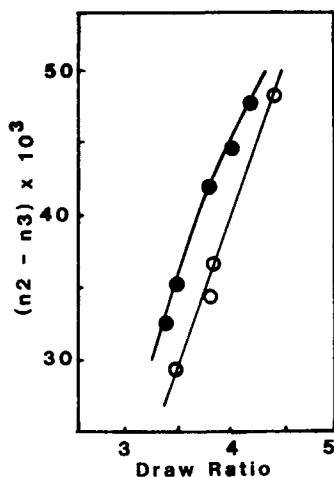


Fig. 6. Variation of the planar birefringence with the plateau draw ratio at 97°C at the beginning of the plateau (O) and after a plateau of 30 s (●).

the crystallinity increases as shown in Figure 5, whatever the plateau draw ratio. This effect is well known in the case of annealing at constant length.<sup>23,24</sup>

The planar birefringence  $n_2 - n_3$  is slightly higher after a long plateau (Fig. 6), and this is probably due to the increase of crystallinity, knowing that, in the crystallites, the benzene rings lie preferentially in the plane of the film for a uniaxial-planar or a biaxial orientation.<sup>25-29</sup>

The axial birefringence  $n_1 - n_2$  increases along a plateau (Fig. 7), but the reason is the increase of crystallinity because, at the same time, the amorphous orientation is reduced by the chains relaxation (Fig. 8).

All these results demonstrate that a plateau is equivalent to an annealing at constant length: increase of crystallinity and relaxation of the amorphous orientation.

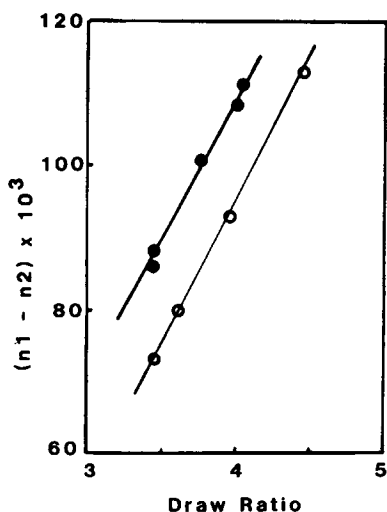


Fig. 7. Variation of the axial birefringence with the plateau draw ratio at 97°C at the beginning of the plateau (O) and after a plateau of 30 s (●).

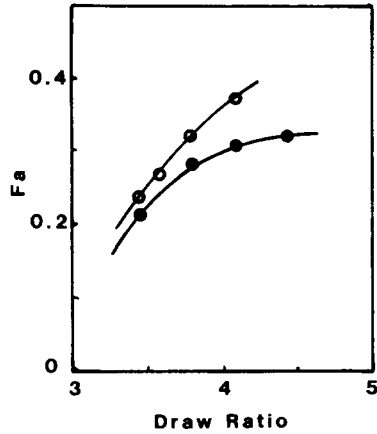


Fig. 8. Variation of the amorphous orientation with the plateau draw ratio at 97°C at the beginning of the plateau (O) and after a plateau of 30 s (●).

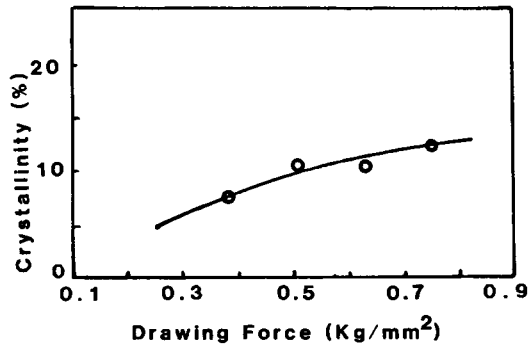


Fig. 9. Evolution of the crystallinity with the drawing force at 80°C at a draw ratio of 3.2.

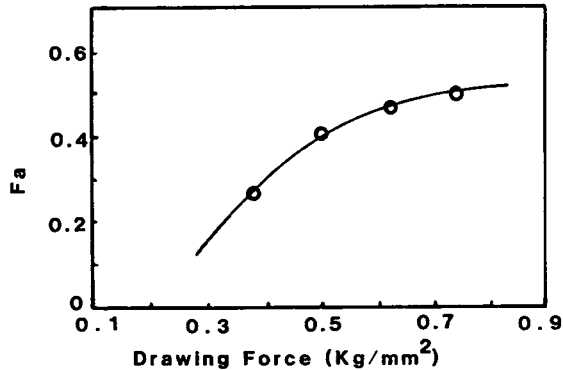


Fig. 10. Evolution of the amorphous orientation with the drawing force at 80°C at a draw ratio of 3.2.

### Influence of the Stretching Force

The influence of the stretching force, i.e., the influence of the path of deformation, in order to reach the same draw ratio (3.2) has been studied at 80°C. The results are gathered in the Figures 9–12.

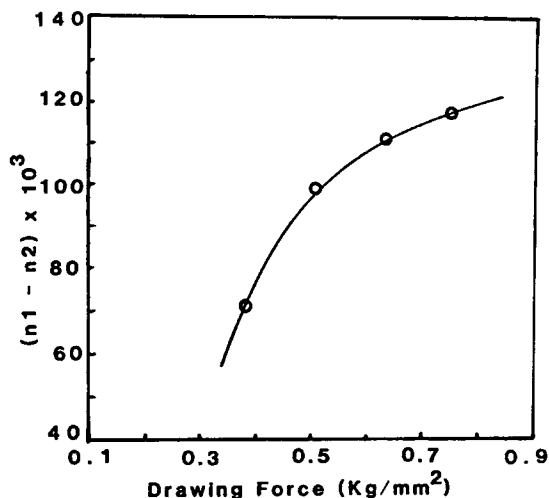


Fig. 11. Evolution of the axial birefringence with the drawing force at 80°C at a draw ratio of 3.2.

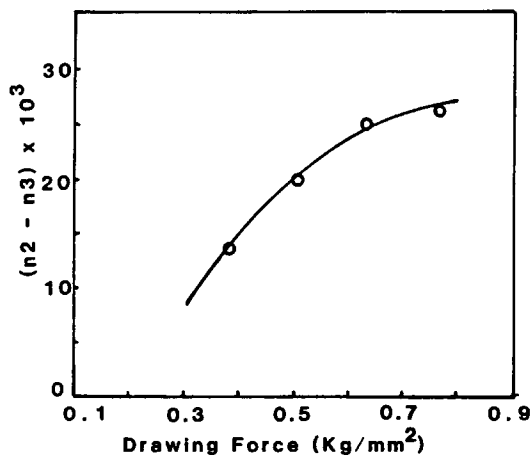


Fig. 12. Evolution of the planar birefringence with the drawing force at 80°C at a draw ratio of 3.2.

The crystallinity increases slowly with the applied load (Fig. 9). As the kinetics of deformation becomes faster when the stretching force increases,<sup>9</sup> the time for crystallization decreases. Moreover, the amorphous orientation increases with the applied load (Fig. 10). Therefore, that means it is an orientation effect which induces the increase of crystallinity.

The axial birefringence increases with the stretching force (Fig. 11) and this is due mainly to the amorphous orientation. The planar birefringence increases also with the applied load (Fig. 12).

#### Influence of the Temperature

The effect of the temperature has been described for drawings at the beginning of the plateau. The axial birefringence is much higher at 80°C than



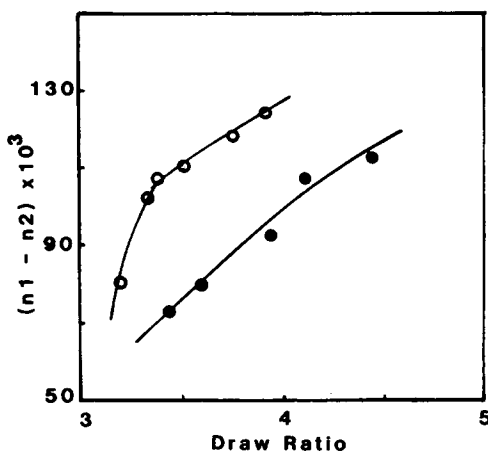


Fig. 13. Variation of the axial birefringence with the plateau draw ratio at 80° (○) and 97°C (●).

at 97°C (Fig. 13), whatever the plateau deformation. The reason is the larger amorphous orientation (Fig. 14) and not an effect of crystallinity (Fig. 15). Indeed, during the stretching, there is a balance between two parameters: temperature and strain rates. A low stretching temperature implies little chain relaxation but, in this case, the strain rate takes low values,<sup>9</sup> leading, on the contrary, to a larger chain relaxation.

So, from Figures 13 and 14, we can conclude that, for stretching under constant load, the temperature is the main parameter which controls the orientation in the film, whatever the strain rates spectrum involved in the

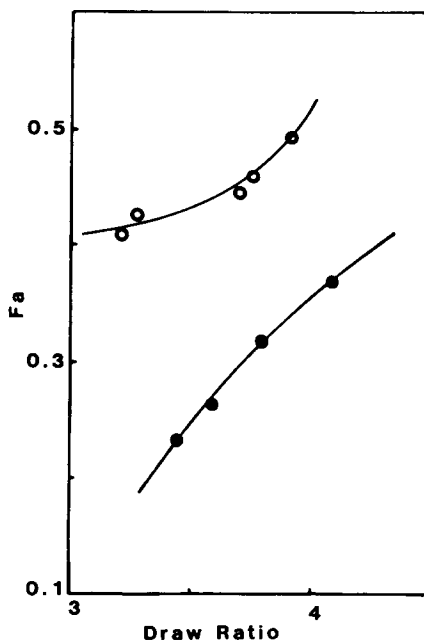


Fig. 14. Variation of the amorphous orientation with the draw ratio at 80° (○) and 97°C (●).

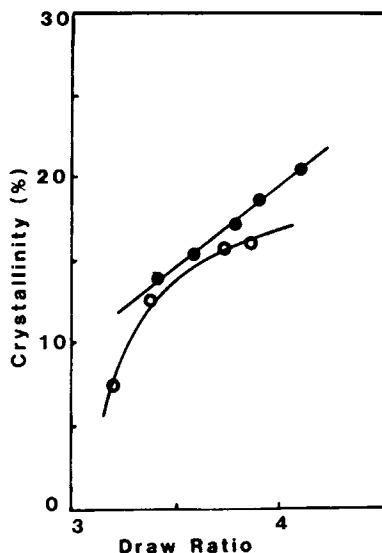


Fig. 15. Variation of the crystallinity with the plateau draw ratio at 80° (○) and 97°C (●).

drawing. In the same deformation range, a high stretching temperature does not induce more crystallinity than a low temperature (Fig. 15). This can be explained by the large strain rates, generated by stretchings at high temperature, which limit the time for crystallization. Another explanation can be the lower amorphous orientation, developed at high temperature, which reduces the entropic effect for strain induced crystallization.

### CONCLUSIONS

This study of drawings under constant load enhanced the influence of stretching conditions on the structure development in PET films:

1. Along a deformation path, the structural properties gradually increase with the draw ratio.
2. A stretching with a long plateau is equivalent to a drawing followed by an annealing at constant length.
3. For a given draw ratio, all the structural properties (crystallinity, amorphous orientation, axial and planar birefringence) increase with the stretching force.
4. At the beginning of a plateau, for a given draw ratio, the degree of crystallinity is independent of the temperature.
5. The stretching temperature is the main parameter which controls the chain orientation, whatever the strain rate spectrum.

### References

1. J. W. Hawthorne and C. J. Heffelfinger, "Polymer films," in *Encyclopedia of Polymer Science and Technology*, Wiley, New York, 1969, Vol. 11.
2. C. J. Heffelfinger and P. G. Schmidt, *J. Appl. Polym. Sci.*, **9**, 2661 (1965).
3. J. Purvis, D. I. Bower, and I. M. Ward, *Polymer*, **14**, 398 (1973).
4. J. H. Nobbs, D. I. Bower, I. M. Ward, and D. Patterson, *Polymer*, **15**, 287 (1974).

5. J. H. Nobbs, D. I. Bower, and I. M. Ward, *Polymer*, **17**, 25 (1976).
6. J. Purvis and D. I. Bower, *J. Polym. Sci., Polym. Phys. Ed.*, **14**, 1461 (1976).
7. J. H. Nobbs, D. I. Bower, and I. M. Ward, *J. Polym. Sci., Polym. Phys. Ed.*, **17**, 259 (1979).
8. T. Matsuo, *Sen'i Gakkaishi*, **24** 366 (1968).
9. G. Le Bourvellec, J. Beautemps, and J. P. Jarry, *J. Appl. Polym. Sci.*, **39**, 319 (1990)  
(Part I).
10. R. J. Samuels, *Structural Polymer Properties*, Wiley, New York, 1974.
11. R. J. Gaylord, *Polym. Lett.*, **13**, 337 (1975).
12. S. R. Padibjo and I. M. Ward, *Polymer*, **24**, 1103 (1983).
13. G. M. Bhatt and J. P. Bell, *J. Polym. Sci., Polym. Phys. Ed.*, **14**, 575 (1976).
14. J. H. Dumbleton, *J. Polym. Sci. A-2*, **6**, 795 (1968).
15. R. J. Samuels, *J. Polym. Sci. A-2*, **9**, 781 (1972).
16. V. B. Gupta and S. Kumar, *J. Appl. Polym. Sci.*, **26**, 1865 (1981).
17. F. Rietsch and B. Jasse, *Polym. Bull.*, **11**, 287 (1984).
18. A. J. De Vries, C. Bonnebat, and J. Beautemps, *J. Polym. Sci., Polym. Symp.*, **58**, 109 (1977).
19. G. Le Bourvellec, doctoral thesis, Univ. of Paris 6, 1984.
20. B. Wunderlich, *Macromolecular Physics*, Academic, New York, 1973, Vol. 1.
21. G. Farrow and I. M. Ward, *Polymer*, **1**, 330 (1960).
22. G. Le Bourvellec, L. Monnerie, and J. P. Jarry, *Polymer*, **27**, 856 (1986).
23. G. Bragato and G. Gianotti, *Eur. Polym. J.*, **19**, 803 (1983).
24. G. Le Bourvellec, L. Monnerie, and J. P. Jarry, *Polymer*, **28**, 1712 (1987).
25. N. Brown, R. A. Duckett, and I. M. Ward, *Phil. Mag.*, **18**, 483 (1968).
26. C. J. Heffelfinger and R. C. Burton, *J. Polym. Sci.*, **47**, 289 (1960).
27. D. A. Jarvis, I. J. Hutchinson, D. I. Bower, and I. M. Ward, *Polymer*, **21**, 41 (1980).
28. M. Cakmak, J. L. White, and J. E. Spruiell, *J. Polym. Eng.*, **6**, 291 (1986).
29. P. M. Henrichs, *Macromolecules*, **20**, 2099 (1987).

Received October 18, 1988

Accepted November 22, 1988